Mixed-metal Carbido Carbonyl Clusters. Part 3.[1] Synthesis and Structural Characterization of $[Rh_6C(CO)_{15}\{Ag(NCMe)\}_2]\cdot 0.5MeOH$, $[Rh_6C(CO)_{15}\{M(PPh_3)\}_2]$ (M = Cu, Ag, or Au), and of the Anion $[Rh_6C(CO)_{15}\{Au(PPh_3)\}]^-$ as its PPh_4^+ Salt‡

Alessandro Fumagalli * **and Secondo Martinengo**
Centro C.N.R. per la Sintesi e la Struttura dei Composti dei Metalli di Transizione nei Bassi Stati di Ossidazione, Via G. Venezian 21, 20133 Milano, Italy
Vincenzo G. Albano† **and Dario Braga**
Dipartimento di Chimica 'G. Ciamician' dell'Universita', Via F. Selmi 2, 40126 Bologna, Italy

The new mixed-metal carbido carbonyl clusters $[Rh_6C(CO)_{15}\{Ag(NCMe)\}_2]$ (**1**), $[Rh_6C(CO)_{15}\{M(PPh_3)\}_2]$ [M = Ag (**2**), Cu (**3**), or Au (**5**)], and $[Rh_6C(CO)_{15}\{Au(PPh_3)\}]^-$ (**4**) have been obtained by reaction in MeOH solution of $[Rh_6C(CO)_{15}]^{2-}$ with $AgBF_4$ (in the presence of MeCN), $[\{MCl(PPh_3)\}_4]$ (M = Cu or Ag), or $[AuCl(PPh_3)]$. Their molecular structures have been determined by single-crystal *X*-ray diffractometry: (**1**), monoclinic, space group *C*2/*c*, *a* = 18.110(3), *b* = 10.455(3), *c* = 20.553(4) Å, β = 125.99(1)°, and *Z* = 4; (**2**), triclinic, space group $P\bar{1}$, *a* = 11.397(3), *b* = 16.519(2), *c* = 16.879(3) Å, α = 116.07(1), β = 98.86(2), γ = 87.77(2)°, and *Z* = 2; (**3**), triclinic, space group $P\bar{1}$, *a* = 11.474(3), *b* = 16.012(9), *c* = 16.688(4) Å, α = 114.25(3), β = 97.82(2), γ = 89.59(4)°, and *Z* = 2; (**4**), monoclinic, space group $P2_1/c$, *a* = 23.009(3), *b* = 14.583(2), *c* = 36.726(4) Å, β = 97.54(1)°, *Z* = 8; (**5**), triclinic, space group $P\bar{1}$, *a* = 11.438(1), *b* = 16.330(7), *c* = 16.813(2) Å, α = 115.58(2), β = 98.68(1), γ = 88.37(2)°, and *Z* = 2. The structural analysis shows that the heterometallic ligands selectively cap one [(**4**)] or both [(**1**)—(**3**), (**5**)] triangular faces of the Rh_6 prismatic framework leaving the CO-ligand stereogeometry almost unaltered. Differences in the heterometallic interactions established by the various metal fragments are discussed.

We have already reported that the hexanuclear prismatic carbido-carbonyl cluster $[Rh_6C(CO)_{15}]^{2-}$ (ref. 2) undergoes electrophilic attack from a variety of metal fragments such as $[Cu(NCMe)_4]^+$,[3] $[Rh(CO)_2(NCMe)_2]^+$,[4] Ag^+, and $[M(PEt_3)]^+$ (M = Ag or Au).[1] Several of these derivatives have been characterized by single-crystal *X*-ray diffraction and multinuclear n.m.r. studies, showing that they share a relevant feature: the interaction of the hetero(homo)metallic fragments with the prismatic dianion always implies selective capping of one or both triangular faces and leaves the overall CO-ligand stereogeometry almost unchanged.

In the case of Ag^+, although n.m.r. data evidenced formation in solution of a series of oligomers, among which $[Ag_n\{Rh_6C(CO)_{15}\}_2]^{(4-n)-}$ (*n* = 1 or 3) and $[Ag_n\{Rh_6C(CO)_{15}\}_3]^{(6-n)-}$ (*n* = 2 or 4) were identified, only the dimeric species $[Ag\{Rh_6C(CO)_{15}\}_2]^{3-}$ could be isolated and characterized in the solid state.[1]

In order to extend the structural characterization to other species and to achieve a better understanding of the heteroatomic metal–metal interactions governing these systems, we attempted the reaction of $[Rh_6C(CO)_{15}]^{2-}$ with other derivatives of Cu^I, Ag^I, and Au^I under different conditions. We are now able to report the synthesis and crystallographic characterization of a series of neutral diadducts, which includes $[Rh_6C(CO)_{15}\{Ag(NCMe)\}_2]$ (**1**), $[Rh_6C(CO)_{15}\{M(PPh_3)\}_2]$ [M = Ag (**2**), Cu (**3**), or Au (**5**)], and of the anion $[Rh_6C(CO)_{15}\{Au(PPh_3)\}]^-$ (**4**). This last can be regarded as the first example of a monocapped derivative in this family, although capping of only one triangular face was also observed in the more complicated metal polyhedra of $[Ag\{Rh_6C(CO)_{15}\}_2]^{3-}$ (ref. 1) and $[Rh_{14}C_2(CO)_{33}]^{2-}$,[4] which contain two prismatic units joined together by an Ag atom and by a $Rh_2(CO)_3$ fragment, respectively. Species (**2**), (**3**), and (**5**) are isostructural and isomorphous, while (**1**) is isomorphous with the previously reported $[Rh_6C(CO)_{15}\{Cu(NCMe)\}_2]$ (**6**).[3]

Results and Discussion

Synthesis and Chemical Characterization of Complexes (**1**)—(**3**).—The reaction of $[Rh_6C(CO)_{15}]^{2-}$ with silver(I) derivatives has been found to yield several products, often as a mixture, the nature of which depends essentially on the molar ratio of the two reactants, the solvent, and the nature of the silver derivative.

The reaction in propan-2-ol of equimolar amounts of $AgBF_4$ and $K_2[Rh_6C(CO)_{15}]$ gives immediate precipitation of a fine yellow powder; analysis of this product gives a Ag:Rh ratio of 1:6, suggesting $K[AgRh_6C(CO)_{15}]\cdot n$solvent as a possible formulation. The product, soluble in acetone, exhibits two i.r. absorptions in the region of terminal CO (2 034s and 2 018s cm^{-1}) and two in the region of bridging CO (1 889ms and 1 840m cm^{-1}), perhaps due to a mixture of products. No precipitate is formed if the solvent is methanol, and a fairly stable yellow solution, showing the same i.r. bands as above, is obtained. Addition of $[N(PPh_3)_2]_2SO_4$ to this solution gives a rusty-red amorphous precipitate; its unexpected insolubility in all common solvents, however, appears in contrast with a simple formulation such as $[N(PPh_3)_2][AgRh_6C(CO)_{15}]$, deduced from elemental analysis, and supports the hypothesis of a polymeric (and therefore polyanionic) species. The i.r. spectrum in Nujol mull of this product shows broad bands at 2 020s, 1 875ms, and 1 825m cm^{-1}.

When Ag^+ and $[Rh_6C(CO)_{15}]^{2-}$ react in a 2:1 molar ratio yellow reddish opalescent solutions are obtained both in

---

* For correspondence on synthesis and chemical characterization.

† For correspondence on structural characterization.

‡ *Supplementary data available:* see Instructions for Authors, *J. Chem. Soc., Dalton Trans.*, 1988, Issue 1, pp. xvii—xx.

methanol and propan-2-ol. In the latter solvent, however, formation of the above described yellow precipitate is observed first, at the ratio 1 : 1, followed by redissolution upon addition of a second mol of $AgBF_4$. The i.r. spectra appear to be the same in both cases, with bands at *ca.* 2 025s, 1 880ms, and 1 840m cm^{-1}. The product can be recovered as a yellow precipitate from the propan-2-ol solution by addition of toluene. It is insoluble in CH_2Cl_2 and fairly soluble in acetone, methanol, and propan-2-ol. Elemental analysis gives the expected internal Ag:Rh ratio of 1 : 3, but any attempt to crystallize this product failed, due to slow decomposition in solution to red insoluble materials.

These results, particularly the instability in solution and the isolation of the insoluble $N(PPh_3)_2$ salt from methanol, are in accord with previous n.m.r. observations on the existence, around the Ag:Rh_6 ratio 1 : 1, of polymers of the $[AgRh_6C(CO)_{15}]^-$ unit which, on subsequent addition of Ag^+, undergo progressive fragmentation to yield eventually $[Ag_2Rh_6C(CO)_{15}]$. The complex behaviour of the Ag^+–$[Rh_6C(CO)_{15}]^{2-}$ system can be explained by taking into account the unusual properties of the $[AgRh_6C(CO)_{15}]^-$ adduct first formed by reaction of Ag^+ with $[Rh_6C(CO)_{15}]^{2-}$. This adduct can be regarded as a molecular ion bearing on one side an electron-acceptor centre (the co-ordinatively unsaturated silver atom) and on the opposite side an electron-donor centre (the unoccupied triangular face of the Rh_6 prism, on which some negative charge is localized). Polymerization of the $[AgRh_6C(CO)_{15}]^-$ units can thus result from intermolecular donor–acceptor interactions. Chain terminations occur both at a Ag:Rh_6 ratio lower than one by reaction with $[Rh_6C(CO)_{15}]^{2-}$, and at higher than one by reaction with Ag^+.

In basic solvents, however, the silver atom of the $[AgRh_6C(CO)_{15}]^-$ adduct can co-ordinate the solvent itself and whether chain formation will occur depends on the relative ability of the solvent and the Rh_3 prism face to bond to silver. The results described above and previously reported n.m.r. observations indicate that neither methanol and propan-2-ol nor acetone is effective in preventing polymer formation. In the presence of some MeCN (5—10% v/v), however, it has been possible to isolate, at an Ag:Rh_6 ratio of 2 : 1, the neutral species $[Rh_6C(CO)_{15}\{Ag(NCMe)\}_2]$, analogous to the previously reported $[Rh_6C(CO)_{15}\{Cu(NCMe)\}_2]$.[3] This silver derivative, however, when dissolved in pure thf (not doped with MeCN), again decomposes.

The sensitivity to solvents, and the facile fragmentation the polymers undergo on simple addition of more Ag^+, indicate that all the species involved in the Ag^+–$[Rh_6C(CO)_{15}]^{2-}$ adduct formation are related by equilibria which are easily shifted in either direction by slight modifications of the reaction conditions. Formation of oligomers or polymers is prevented only when strong ligands such as PPh_3 are bonded to silver. In this case we have isolated, by reaction of $[Rh_6C(CO)_{15}]^{2-}$ with $[\{MCl(PPh_3)\}_4]$ (M = Cu or Ag), the derivatives $[Rh_6C(CO)_{15}\{M(PPh_3)\}_2]$ (M = Cu or Ag) which are stable both in solution and in crystalline form. The copper derivative is somewhat less soluble of that of Ag in tetrahydrofuran (thf); both are sparingly soluble in acetone but decompose in MeCN with extraction of $[M(PPh_3)]^+$ and formation of what we believe to be the monoanionic derivatives $[Rh_6C(CO)_{15}\{M(PPh_3)\}]^-$. We are presently investigating these monoanionic species but, so far, have succeeded in the isolation of only the gold analogue (see below).

All silver species were found to be light-sensitive, even in the solid state, as shown by progressive darkening of originally yellow samples; this makes advisable quick manipulations in dim light and storage in the dark.

The i.r. spectra of the reported species in the carbonyl-stretching region are all very similar, and compare well (Table 1) with that of $[Rh_6C(CO)_{15}\{Cu(NCMe)\}_2]$.[3] The i.r. spectrum in thf of $[Rh_6C(CO)_{15}\{Ag(PPh_3)\}_2]$ is reported as a reference in Figure 1.

Table 1. Infrared CO stretching (cm^{-1}) of $[Rh_6C(CO)_{15}(ML)_2]$ (M = Cu, Ag, or Au; L = NCMe or PPh_3) and $[Rh_6C(CO)_{15}\{Au(PPh_3)\}]^-$ in thf solution

$[Rh_6C(CO)_{15}\{Cu(NCMe)\}_2]$	2 027s,[a] 1 995w (sh), 1 878s, 1 850m
$[Rh_6C(CO)_{15}\{Ag(NCMe)\}_2]$	2 020s, 1 879s, 1 845m
$[Rh_6C(CO)_{15}\{Cu(PPh_3)\}_2]$	2 033s, 1 888s, 1 867m
$[Rh_6C(CO)_{15}\{Ag(PPh_3)\}_2]$	2 028s, 1 886s, 1 859m
$[Rh_6C(CO)_{15}\{Au(PPh_3)\}_2]$	2 036s, 1 890s, 1 859m
$[Rh_6C(CO)_{15}\{Au(PPh_3)\}]^-$	2 044vw, 2 014s, 1 868s, 1 836m
$[Rh_6C(CO)_{15}]^{2-}$[b]	1 988vs, 1 982 (sh), 1 840s, 1 810mw

[a] This band was erroneously reported in the previous work as 2 070 cm^{-1}.[3] [b] As the $[PPh_4]^+$ salt.

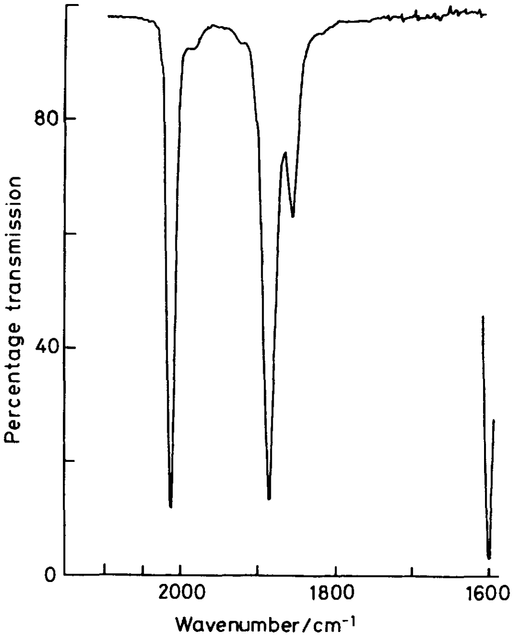

Figure 1. I.r. spectrum of $[Rh_6C(CO)_{15}\{Ag(PPh_3)\}_2]$ in thf solution

Synthesis and Chemical Characterization of Complexes (**4**), *and* (**5**).—The reaction of $[Rh_6C(CO)_{15}]^{2-}$ with $[AuCl(PPh_3)]$ yields $[Rh_6C(CO)_{15}\{Au(PPh_3)\}]^-$ (**4**) and $[Rh_6C(CO)_{15}\{Au(PPh_3)\}_2]$ (**5**), according to the two-step reaction (1). No other product has been detected by i.r. spectroscopy.

$$[Rh_6C(CO)_{15}]^{2-} \xrightarrow{[AuCl(PPh_3)]} [Rh_6C(CO)_{15}\{Au(PPh_3)\}]^- \xrightarrow{[AuCl(PPh_3)]} [Rh_6C(CO)_{15}\{Au(PPh_3)\}_2] \quad (1)$$

Compound (**5**) can be obtained almost quantitatively as a fine bright yellow precipitate by treating $K_2[Rh_6C(CO)_{15}]$ in MeOH (or MeOH–$CHCl_3$ mixtures) with $[AuCl(PPh_3)]$ in the molar ratio 1 : 2. As mentioned above, the isolation of monoanionic species is more difficult. Treatment of $K_2[Rh_6C(CO)_{15}]$ in MeOH with $[AuCl(PPh_3)]$ in slight excess over a 1 : 1 molar ratio gives i.r. evidence of essentially the monoanionic derivative (**4**) while some (**5**) is precipitated. From this solution, by slow diffusion of propan-2-ol containing some $[PPh_4]Cl$, a few crystals of (**4**), suitable for *X*-ray diffraction studies, were obtained. However, this product and others obtained similarly by metathesis with bulky cations contain amounts of co-precipitated $[Rh_6C(CO)_{15}]^{2-}$. On the other hand, the reaction of $[PPh_4]_2[Rh_6C(CO)_{15}]$ with $[AuCl(PPh_3)]$ in thf at a 1:1 molar ratio is not complete and a 1:2 ratio is required to force the formation of $[Rh_6C(CO)_{15}\{Au(PPh_3)\}]^-$; addition of propan-2-ol to this solution gives precipitation of $[Rh_6C(CO)_{15}\{Au(PPh_3)\}_2]$. This behaviour can be explained with the existence of equilibria dependent on the solvent, on the relative solubilities of the three cluster species involved, and on the presence of chloride ions (see later). The best method of preparation of (**4**) is to operate in the absence of chloride ions. This has been achieved by mixing in thf equimolar amounts of $[PPh_4]_2[Rh_6C(CO)_{15}]$ and $[Rh_6C(CO)_{15}\{Au(PPh_3)\}_2]$: in a short time complete equilibration to $[PPh_4][Rh_6C(CO)_{15}\{Au(PPh_3)\}]$ is observed. The product can therefore be recovered easily.

Compound (**4**) is well soluble and stable in thf while compound (**5**) is moderately soluble with some dissociation to the monoanionic species, as evidenced by the slow appearance in the i.r. spectrum of two very weak shoulders which could be assigned to (**4**) by subtractive i.r. techniques. The equilibrium is however soon achieved and no further increase in the shoulders is observed. In acetone and MeCN, where compound (**5**) is sparingly soluble, the dissolved part is completely dissociated into $[Au(PPh_3)]^+$ and (**4**).

Both (**4**) and (**5**) react with Cl^- ions in excess in thf releasing $[AuCl(PPh_3)]$ to give $[Rh_6C(CO)_{15}]^{2-}$ or (**4**), respectively; I^- is even more effective and causes formation of $[Rh_6C(CO)_{15}]^{2-}$ also starting from (**5**).

As observed for the silver analogues, these species are slightly light-sensitive, even in the solid state, as shown by progressive darkening of originally yellow samples.

The i.r. spectrum in the carbonyl-stretching region of $[PPh_4][Rh_6C(CO)_{15}\{Au(PPh_3)\}]$ in thf solution is reported in Figure 2. Stretching frequencies for both (**4**) and (**5**) are listed in Table 1; they show the expected shift to higher wavenumbers in going from $[Rh_6C(CO)_{15}]^{2-}$ to the monoanion (**4**) and to the neutral species (**5**).

Structural Characterization.—The structures of complexes (**1**)—(**3**) and (**5**) are all based on a trigonal-prismatic framework of Rh atoms capped on both triangular faces by the heteroatoms, which bear a linear acetonitrile ligand in (**1**) and a PPh_3 ligand in (**2**), (**3**), and (**5**). In the case of (**4**) the Rh_6 core is monocapped by an $Au(PPh_3)$ fragment. The prismatic framework accommodates the interstitial C atom. The CO ligand stereogeometry is kept almost unaltered with respect to the parent dianion, showing one CO terminally bound to each Rh atom and bridging CO groups on all prism edges. The structures of complexes (**2**) and (**4**) are reported in Figures 3 and 4, respectively.

The species (**1**) is isostructural with the already reported (**6**),[3] and their crystals are isomorphous. Therefore both molecules have D_{3h} idealized symmetry and retain in the crystal a two-fold axis passing through the carbide atom and one of the interbasal bridging CO groups [C(8)–O(8)]. In the case of (**2**), (**3**), and (**5**), which also are isostructural and isomorphous, the symmetry is lowered by the phenyl-group conformations, and the molecules are asymmetric in the crystals.

A comparative analysis of the more relevant average structural parameters for the dianion $[Rh_6C(CO)_{15}]^{2-}$, for (**6**), and for all species discussed herein is reported in Table 2. Relevant bond distances and angles for (**1**) are given in Table 3, those of the isomorphous (**2**), (**3**), and (**5**) in Table 4; mean values of the structural parameters in the two independent anions found in

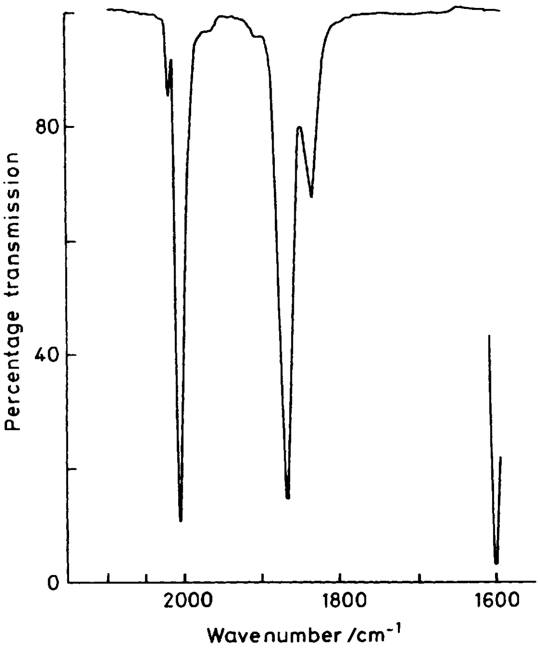

Figure 2. I.r. spectrum of $[PPh_4][Rh_6C(CO)_{15}\{Au(PPh_3)\}]$ in thf solution

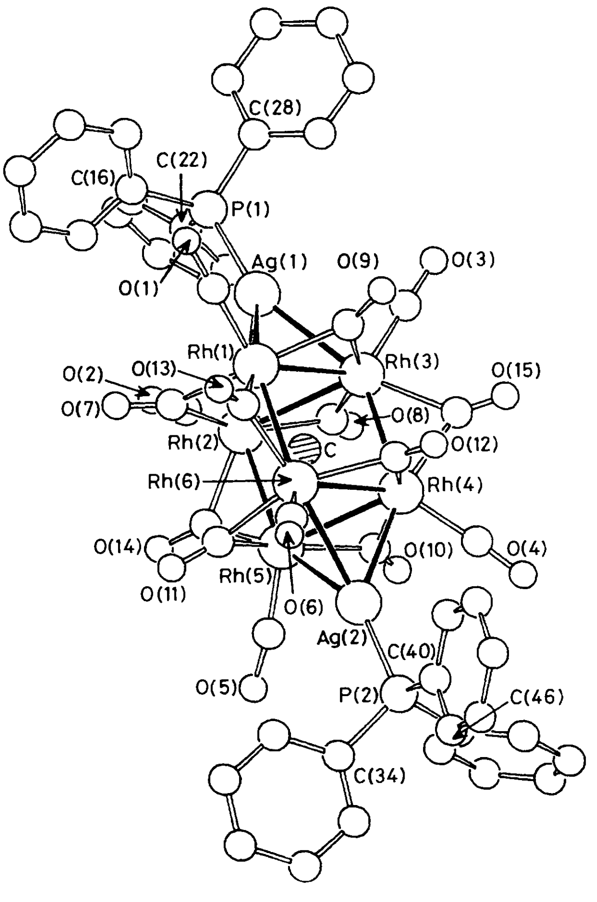

Figure 3. The structure of $[Rh_6C(CO)_{15}\{Ag(PPh_3)\}_2]$. Carbon atoms of the CO groups bear the same numbering as the O atoms

Table 2. Comparison of average bond lengths (Å) and angles (°)

	Rh–Rh				Rh–C–O			
	basal	interbasal	Rh–M	Rh–C	terminal	bridge, basal	bridge, interbasal	Rh–C–O terminal
$[Rh_6C(CO)_{15}]^{2-}$	2.776(3)	2.817(2)	—	2.134(6)	1.89(1) 1.13(1)	2.12(1) 1.14(2)	2.04(1) 1.17(2)	178(1)
$[Rh_6C(CO)_{15}\{Ag(NCMe)\}_2]$	2.775(1)	2.805(4)	2.822(1)	2.13(1)	1.91(1) 1.11(1)	2.13(1) 1.16(1)	2.05(1) 1.15(1)	175(1)
$[Rh_6C(CO)_{15}\{Ag(PPh_3)\}_2]$	2.785(1)	2.808(1)	2.823(1)	2.13(1)	1.92(1) 1.11(1)	2.14(1) 1.13(1)	2.06(1) 1.13(1)	176(1)
$[Rh_6C(CO)_{15}\{Cu(PPh_3)\}_2]$	2.768(1)	2.813(1)	2.662(1)	2.129(6)	1.910(8) 1.13(10)	2.133(6) 1.139(8)	2.071(7) 1.146(8)	176(1)
$[Rh_6C(CO)_{15}\{Cu(NCMe)\}_2]$	2.765(1)	2.810(1)	2.660(1)	2.127(3)	1.88(1) 1.18(1)	2.13(1) 1.17(1)	2.05(1) 1.18(1)	174(1)
$[Rh_6C(CO)_{15}\{Au(PPh_3)\}]^-$	2.766(4)[a] 2.772(4)[b]	2.807(3)	2.820(3)	2.17(3) 2.09(3)	*c*	*c*	*c*	*c*
$[Rh_6C(CO)_{15}\{Au(PPh_3)\}_2]$	2.780(1)	2.805(1)	2.824(1)	2.13(1)	1.91(1) 1.13(2)	2.13(1) 1.16(2)	2.07(1) 1.14(2)	176(1)

[a] Capped face. [b] Uncapped face. [c] See Table 5.

Table 3. Relevant bond distances (Å) and angles (°) for complex (**1**)

Rh(1)–Rh(2)	2.775(1)	Rh(3)–C(1)	2.14(1)
Rh(1)–Rh(3)	2.776(1)	Rh(3)–C(2)	2.12(1)
Rh(2)–Rh(3)	2.775(1)	Rh(3)–C(7)	2.05(1)
Rh(2)–Rh(2′)	2.805(2)	Ag–N	2.14(1)
Rh(1)–Rh(3′)	2.805(1)	N–C(9)	1.11(1)
Rh(1)–Ag	2.823(1)	C(9)–C(10)	1.44(2)
Rh(2)–Ag	2.821(1)	Ag–C(1)	3.24(1)
Rh(3)–Ag	2.821(1)	Ag–C(2)	3.24(1)
Rh(1)–C(0)	2.12(1)	Ag–C(3)	3.25(1)
Rh(2)–C(0)	2.14(1)	Ag–C(4)	3.05(1)
Rh(3)–C(0)	2.13(1)	Ag–C(5)	3.06(1)
Rh(1)–C(4)	1.91(1)	Ag–C(6)	3.08(1)
Rh(1)–C(2)	2.14(1)	C(1)–O(1)	1.15(1)
Rh(1)–C(3)	2.14(1)	C(2)–O(2)	1.17(1)
Rh(1)–C(7′)	2.06(1)	C(3)–O(3)	1.16(1)
Rh(2)–C(5)	1.91(1)	C(4)–O(4)	1.12(1)
Rh(2)–C(1)	2.14(1)	C(5)–O(5)	1.13(1)
Rh(2)–C(3)	2.12(1)	C(6)–O(6)	1.09(1)
Rh(2)–C(8)	2.05(1)	C(7)–O(7)	1.14(1)
Rh(3)–C(6)	1.92(1)	C(8)–O(8)	1.16(2)
Rh(2)–C(1)–O(1)	139(1)	Rh(2)–C(5)–O(5)	175(1)
Rh(3)–C(1)–O(1)	140(1)	Rh(3)–C(6)–O(6)	177(1)
Rh(1)–C(2)–O(2)	138(1)	Rh(3)–C(7)–O(7)	138(1)
Rh(3)–C(2)–O(2)	140(1)	Rh(1′)–C(7)–O(7)	135(1)
Rh(1)–C(3)–O(3)	138(1)	Rh(2)–C(8)–O(8)	137(1)
Rh(2)–C(3)–O(3)	140(1)	Ag–N–C(9)	179(1)
Rh(1)–C(4)–O(4)	174(1)	N–C(9)–C(10)	178(1)

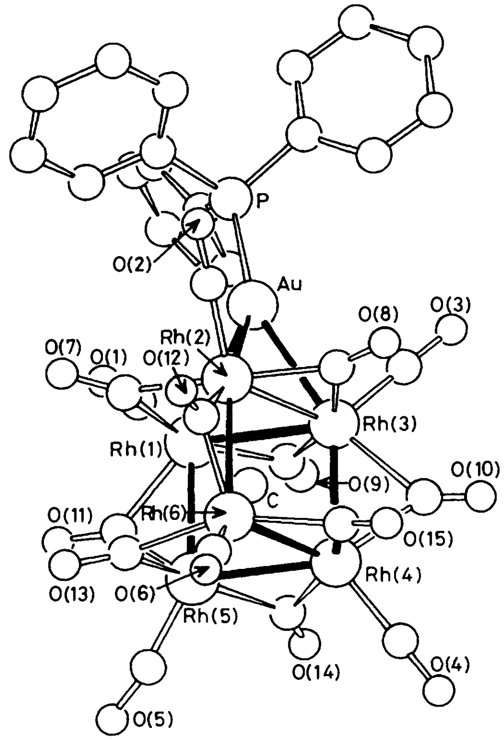

Figure 4. The structure of the anion $[Rh_6C(CO)_{15}\{Au(PPh_3)\}]^-$ Details as in Figure 3

the crystal unit cell of (**4**) (see Experimental section) are reported in Table 5.

The Rh–Ag bond lengths [mean 2.822(1) and 2.823(1) Å in (**1**) and (**2**) respectively] are as expected longer than the Rh–Cu ones [mean 2.662(1) and 2.660(1) Å in (**3**) and (**6**), respectively], while strictly comparable with the average Rh–Au distances in (**4**) and (**5**) [2.820(3) and 2.824(1) Å, respectively]. All mean values appear to be in good agreement with the sum of the metallic radii.[5] A comparison of the average Rh–Ag bond lengths in complexes (**1**) and (**2**) with the average distance found in $[Ag\{Rh_6C(CO)_{15}\}_2]^{3-}$ [2.983(1) Å],[1] in which the Ag atom is sandwiched between two staggered Rh_6 prisms, confirms that the longer values in the trianion result from a compromise between attractive cation–anion and repulsive anion–anion interactions.

The Ag atoms in complex (**1**) are located almost exactly over the centre of the triangular faces, thus conforming to the idealized D_{3h} symmetry [Rh–Ag range: 2.821(1)—2.823(1) Å], while the heteroatoms adopt fairly asymmetric positions in (**2**) and (**3**) [range: 2.790(1)—2.861(1) and 2.810(1)—2.823(1) Å for Rh–Ag(1) and Rh–Ag(2); 2.629(1)—2.692(1) and 2.647(1)—2.665(1) for Rh–Cu(1) and Rh–Cu(2), respectively]. Similar considerations apply to the structures of (**4**) and (**5**), which show Rh–Au bonds ranging from 2.749(3) to 2.860(3) and from 2.781(1) to 2.863(1) Å respectively. This fact, together with the different degree of asymmetry shown by the two sets of M–Rh interactions in all $M(PPh_3)$ derivatives, can be accounted for in terms of asymmetry of the packing forces, which are less uniform around the bulky and flexible PPh_3 ligands than

Table 4. Relevant bond distances (Å) and angles (°) for complexes (**2**), (**3**), and (**5**)

	(**2**) M = Ag	(**3**) M = Cu	(**5**) M = Au		(**2**) M = Ag	(**3**) M = Cu	(**5**) M = Au
Rh(1)–Rh(2)	2.793(1)	2.781(1)	2.795(1)	Rh(1)–C(1)	1.92(1)	1.92(1)	1.90(2)
Rh(1)–Rh(3)	2.777(1)	2.767(1)	2.770(1)	Rh(2)–C(2)	1.92(1)	1.91(1)	1.92(2)
Rh(2)–Rh(3)	2.788(1)	2.768(1)	2.784(1)	Rh(3)–C(3)	1.93(1)	1.91(1)	1.92(1)
Rh(4)–Rh(5)	2.767(1)	2.752(1)	2.762(1)	Rh(4)–C(4)	1.94(1)	1.91(1)	1.91(2)
Rh(4)–Rh(6)	2.790(1)	2.768(1)	2.783(1)	Rh(5)–C(5)	1.92(1)	1.90(1)	1.91(1)
Rh(5)–Rh(6)	2.793(1)	2.772(1)	2.784(1)	Rh(6)–C(6)	1.91(1)	1.91(1)	1.89(2)
Rh(1)–Rh(6)	2.828(1)	2.830(1)	2.824(2)	Rh(1)–C(7)	2.12(1)	2.13(1)	2.09(2)
Rh(2)–Rh(5)	2.795(1)	2.804(1)	2.793(2)	Rh(2)–C(7)	2.18(1)	2.17(1)	2.16(1)
Rh(3)–Rh(4)	2.801(1)	2.806(1)	2.797(2)	Rh(2)–C(8)	2.16(1)	2.15(1)	2.16(1)
Rh(1)–M(1)	2.861(1)	2.692(1)	2.863(1)	Rh(3)–C(8)	2.12(1)	2.11(1)	2.14(2)
Rh(2)–M(1)	2.838(1)	2.687(1)	2.847(1)	Rh(1)–C(9)	2.11(1)	2.10(1)	2.10(1)
Rh(3)–M(1)	2.790(1)	2.629(1)	2.781(1)	Rh(3)–C(9)	2.16(1)	2.16(1)	2.16(1)
Rh(4)–M(2)	2.823(1)	2.647(1)	2.821(1)	Rh(4)–C(10)	2.14(1)	2.14(1)	2.12(1)
Rh(5)–M(2)	2.814(1)	2.665(1)	2.816(1)	Rh(5)–C(10)	2.14(1)	2.13(1)	2.11(1)
Rh(6)–M(2)	2.810(1)	2.651(1)	2.813(1)	Rh(5)–C(11)	2.16(1)	2.15(1)	2.14(1)
Rh(1)–C	2.142(6)	2.131(6)	2.14(1)	Rh(6)–C(11)	2.13(1)	2.11(1)	2.12(1)
Rh(2)–C	2.119(8)	2.128(7)	2.11(1)	Rh(4)–C(12)	2.14(1)	2.13(1)	2.14(1)
Rh(3)–C	2.119(5)	2.115(5)	2.15(1)	Rh(6)–C(12)	2.13(1)	2.12(1)	2.10(1)
Rh(4)–C	2.133(7)	2.129(6)	2.15(1)	Rh(1)–C(13)	2.07(1)	2.07(1)	2.06(1)
Rh(5)–C	2.148(6)	2.137(5)	2.12(1)	Rh(6)–C(13)	2.05(1)	2.07(1)	2.08(1)
Rh(6)–C	2.144(6)	2.135(5)	2.12(1)	Rh(2)–C(14)	2.05(1)	2.07(1)	2.07(1)
M(1)–P(1)	2.383(3)	2.204(2)	2.269(4)	Rh(5)–C(14)	2.06(1)	2.07(1)	2.06(2)
M(2)–P(2)	2.369(3)	2.191(2)	2.262(4)	Rh(3)–C(15)	2.06(1)	2.08(1)	2.08(2)
C(1)–O(1)	1.12(1)	1.13(1)	1.14(2)	Rh(4)–C(15)	2.06(1)	2.06(1)	2.05(1)
C(2)–O(2)	1.11(1)	1.13(1)	1.14(2)	M(1) ··· C(1)	3.10(1)	3.041(1)	3.12(1)
C(3)–O(3)	1.12(1)	1.13(1)	1.11(2)	M(1) ··· C(2)	3.12(1)	3.058(1)	3.15(1)
C(4)–O(4)	1.09(1)	1.14(1)	1.13(2)	M(1) ··· C(3)	3.01(1)	2.954(1)	3.03(1)
C(5)–O(5)	1.12(1)	1.14(1)	1.13(2)	M(2) ··· C(4)	3.03(1)	2.896(1)	3.01(1)
C(6)–O(6)	1.12(1)	1.13(1)	1.14(2)	M(2) ··· C(5)	3.05(1)	2.990(1)	3.05(1)
C(7)–O(7)	1.13(1)	1.12(1)	1.16(2)	M(2) ··· C(6)	3.07(1)	2.996(1)	3.09(1)
C(8)–O(8)	1.13(1)	1.15(1)	1.15(2)				
C(9)–O(9)	1.13(1)	1.14(1)	1.14(2)	P(1)–C_{Ph} (mean)	1.818(5)	1.815(5)	1.81(1)
C(10)–O(10)	1.12(1)	1.14(1)	1.18(2)	P(2)–C_{Ph} (mean)	1.814(5)	1.812(6)	1.81(1)
C(11)–O(11)	1.13(1)	1.14(1)	1.14(1)				
C(12)–O(12)	1.13(1)	1.15(1)	1.17(2)				
C(13)–O(13)	1.14(1)	1.15(1)	1.13(2)				
C(14)–O(14)	1.15(1)	1.15(1)	1.15(2)				
C(15)–O(15)	1.15(1)	1.14(1)	1.13(2)				
Rh(1)–C(1)–O(1)	176(1)	177(1)	178(1)	Rh(4)–C(10)–O(10)	139(1)	138(1)	143(1)
Rh(2)–C(2)–O(2)	175(1)	176(1)	178(1)	Rh(5)–C(10)–O(10)	140(1)	141(1)	140(1)
Rh(3)–C(3)–O(3)	174(1)	176(1)	177(2)	Rh(5)–C(11)–O(11)	136(1)	136(1)	136(1)
Rh(4)–C(4)–O(4)	177(1)	176(1)	175(1)	Rh(6)–C(11)–O(11)	142(1)	142(1)	141(1)
Rh(5)–C(5)–O(5)	175(1)	176(1)	174(2)	Rh(4)–C(12)–O(12)	138(1)	139(1)	136(1)
Rh(6)–C(6)–O(6)	178(1)	176(1)	178(2)	Rh(6)–C(12)–O(12)	140(1)	139(1)	141(1)
Rh(1)–C(7)–O(7)	143(1)	142(1)	142(1)	Rh(1)–C(13)–O(13)	136(1)	137(1)	138(1)
Rh(2)–C(7)–O(7)	136(1)	137(1)	135(1)	Rh(6)–C(13)–O(13)	137(1)	136(1)	136(1)
Rh(2)–C(8)–O(8)	139(1)	139(1)	138(1)	Rh(2)–C(14)–O(14)	137(1)	137(1)	136(1)
Rh(3)–C(8)–O(8)	140(1)	140(1)	140(1)	Rh(5)–C(14)–O(14)	136(1)	137(1)	139(1)
Rh(1)–C(9)–O(9)	141(1)	143(1)	143(1)	Rh(3)–C(15)–O(15)	138(1)	137(1)	136(1)
Rh(3)–C(9)–O(9)	138(1)	136(1)	136(1)	Rh(4)–C(15)–O(15)	136(1)	138(1)	139(1)

around the linear acetonitrile group, also suggesting that these heterometallic interactions are not very strong.

The average Rh–C(carbide) distances in complexes (**1**)—(**3**) and (**5**) [2.13(1) Å] are very similar to that in $[Rh_6C(CO)_{15}]^{2-}$ and show that no substantial changes have occurred in the prismatic moieties. However, while all dicapped species have the carbon atom held in the 'middle' of the trigonal-prismatic cavity, *i.e.* with almost identical distances from each polyhedron vertex, in (**4**) the C atom appears to be 'pushed away' from the capped face. Although the data for (**4**) are rather poor (see Experimental section), the mean Rh–C(carbide) distances show values, in both independent anions, which are longer for the three Rh atoms bonded to Au than for the other three [2.17(3), 2.09(3); and 2.16(3), 2.09(3) Å, respectively]. A similar effect, although accompanied by important distortions of the metal framework, was observed only in the structure $[Rh_{14}C_2(CO)_{33}]^{2-}$ [2.15(1) and 2.11(1) Å, from capped and uncapped faces, respectively],[4] while no effect was observed in $[Ag\{Rh_6C(CO)_{15}\}_2]^{3-}$.[1]

Contacts between the capping metal atoms and the surrounding terminal CO ligands average 3.06(1) Å for Ag ··· CO in both (**1**) and (**2**), 2.99(1) Å for Cu ··· CO in (**3**), and 3.17(4) and 3.08(1) Å for Au ··· CO in (**4**) and (**5**), and are characterized by a slight bending of the ligands [mean Rh–C–O 175(1) in (**1**), 176(1) in (**2**), 176 (1) in (**3**), and 176(1)° in (**5**)]. The fact that the terminal CO groups around the capping atom in $[Ag\{Rh_6C(CO)_{15}\}_2]^{3-}$ exhibit a more significant deviation from linearity [171(1)°] in spite of the longer Ag ··· C contact of 3.17(1) Å suggests that the ligand bending in this latter species

Table 5. Relevant bond distances (Å) and angles (°) for the two crystallographically independent anions of complex (**4**)

Rh(1)–Rh(2)	2.763(4)	Rh(7)–Rh(8)	2.759(4)
Rh(1)–Rh(3)	2.763(4)	Rh(7)–Rh(9)	2.770(3)
Rh(2)–Rh(3)	2.789(3)	Rh(8)–Rh(9)	2.750(4)
Rh(4)–Rh(5)	2.752(4)	Rh(10)–Rh(11)	2.780(4)
Rh(4)–Rh(6)	2.787(3)	Rh(10)–Rh(12)	2.764(4)
Rh(5)–Rh(6)	2.759(4)	Rh(11)–Rh(12)	2.788(4)
Rh(1)–Rh(5)	2.824(4)	Rh(7)–Rh(11)	2.793(4)
Rh(2)–Rh(6)	2.810(4)	Rh(8)–Rh(12)	2.790(4)
Rh(3)–Rh(4)	2.805(4)	Rh(9)–Rh(10)	2.817(4)
Rh(1)–Au(1)	2.847(3)	Rh(7)–Au(2)	2.749(3)
Rh(2)–Au(1)	2.828(3)	Rh(8)–Au(2)	2.827(3)
Rh(3)–Au(1)	2.807(3)	Rh(9)–Au(2)	2.860(3)
Au(1)–P(1)	2.28(1)	Au(2)–P(2)	2.25(1)

Mean values *			
Capped face	Rh–C (terminal)	1.84(3)	1.82(3)
	C–O (terminal)	1.20(4)	1.20(4)
	Rh–C (bridge)	2.05(3)	2.08(3)
	C–O (bridge)	1.20(4)	1.18(4)
	Rh–C (carbide)	2.17(3)	2.16(3)
	P–C	1.82(2)	1.81(2)
Uncapped face	Rh–C (terminal)	1.83(3)	1.82(3)
	C–O (terminal)	1.20(4)	1.21(4)
	Rh–C (bridge)	2.06(3)	2.03(3)
	C–O (bridge)	1.22(4)	1.23(4)
	Rh–C (carbide)	2.09(3)	2.09(3)
Interbasal	Rh–C	2.04(3)	1.98(3)
	C–O	1.18(4)	1.23(4)

* Due to the poor quality of data, only average values are reported for all structural parameters involving the light atoms (see Experimental section); estimated standard deviations (e.s.d.s) on the mean values are in parentheses.

can result from a co-operation of incipient Ag···CO bonding interactions and intramolecular steric pressure between oxygen atoms belonging to the two staggered prismatic moieties.

Bond parameters for the two sets of terminal and bridging CO groups are substantially equivalent in complexes (**1**)—(**3**) and (**5**) (see Table 2). The difference between the values of (**3**) and those reported for (**6**) are not significant and have to be disregarded because in the present study [except in the case of (**4**)] light atoms were refined with full anisotropic thermal motion (see Experimental section) while in (**6**) they were treated isotropically. It has recently been shown[6] that systematic errors are introduced in M–C and C–O distances when light-atom thermal motion is treated isotropically, rendering comparisons meaningless.

It is worth mentioning the difference between the Au(PPh$_3$) and the Cu(NCMe) groupings, which are frequently present in mixed-metal clusters. While the Cu(NCMe) ligand has always been found to give μ_3 co-ordination on metal clusters, the bulkier Au(PPh$_3$) ligand gives also μ co-ordination, very probably in order to reduce contacts with adjacent ligands. This difference has been attributed[7] to the possibility with a co-ordinated copper fragment of accepting electron density into its empty and relatively low-lying p_x and p_y orbitals. These orbitals are too high in energy in the case of Au, so that its bonding geometry is more influenced by the need to optimize non-bonded interactions. Similar considerations might apply to the analogous silver derivatives.

Interestingly, while the copper adducts exhibit small but general shrinkage of all Rh$_6$ prism edges, both silver and gold derivatives show a more significant contraction of the inter-basal distances and almost no effect, if not a slight expansion, in the basal triangles (see Table 2). These effects clearly originate

Table 6. Summary of crystal data and intensity collection parameters[a]

Complex	(**1**)	(**2**)	(**3**)	(**4**)	(**5**)
Formula	$C_{20.5}H_8Ag_2N_2O_{15.5}Rh_6$	$C_{52}H_{30}Ag_2O_{15}P_2Rh_6$	$C_{52}H_{30}Cu_2O_{15}P_2Rh_6$	$C_{58}H_{35}AuO_{15}P_2Rh_6$	$C_{52}H_{30}Au_2O_{15}P_2Rh_6$
M	1 363.5	1 789.9	1 701.3	1 848.3	1 968.1
Crystal size/mm	0.05 × 0.05 × 0.01	0.1 × 0.1 × 0.2	0.15 × 0.09 × 0.1	0.1 × 0.2 × 0.15; 0.1 × 0.15 × 0.15[b]	0.05 × 0.02 × 0.08
System	Monoclinic	Triclinic	Triclinic	Monoclinic	Triclinic
Space group	$C2/c$	$P\bar{1}$	$P\bar{1}$	$P2_1/c$[c]	$P\bar{1}$
a/Å	18.110(3)	11.397(3)	11.474(3)	23.009(3)	11.438(1)
b/Å	10.455(3)	16.519(2)	16.012(9)	14.583(2)	16.330(7)
c/Å	20.553(4)	16.879(3)	16.688(4)	36.726(4)	16.813(2)
α/°		116.07(1)	114.25(3)		115.58(2)
β/°	125.99(1)	98.86(2)	97.82(2)	97.54(1)	98.68(1)
γ/°		87.77(2)	89.59(4)		88.37(2)
U/Å^3	3 148.7	2 818.9	2 765.3	12 216.5	2 793.8
Z	4	2	2	8	2
F(000)	2 448	1 712	1 640	6 632	1 840
D_c/g cm^{-3}	2.88	2.11	2.04	2.00	2.34
μ(Mo-K_α)/cm^{-1}	42.94	24.8	25.95	40.5	70.2
θ range/°	2.5—27	2.5—24	2.5—25	3—20	2.5—23
ω scan width/°	1.3 + 0.35 tan θ	0.8 + 0.35 tan θ	0.9 + 0.35 tan θ	0.8 + 0.35 tan θ	0.65 + 0.35 tan θ
Requested counting $\sigma(I)/I$	0.01	0.01	0.01	0.02	0.01
Maximum scan time/s	120	120	120	150	120
Octants explored in reciprocal space	$\pm h +k +l$	$\pm h \pm k +l$	$\pm h \pm k +l$	$\pm h +k +l$	$\pm h \pm k +l$
Measured reflections	3 704	8 104	10 615	9 570	8 050
Unique observed reflections	1 942	7 049	6 326	4 567	4 122
$[F_o > n\sigma(F_o)]$	$n = 4$	$n = 5$	$n = 5$	$n = 5$	$n = 5$
R, R'[d]	0.035, 0.036	0.067, 0.074	0.029, 0.031	0.077, 0.079	0.033, 0.033
k, g	1.16, 0.0002	1.0, 0.000 39	2.18, 0.000 16	1.0, 0.014	1.46, 0.0005

[a] Details common to all structures: scan mode ω—2θ; pre-scan rate 6° min^{-1}, acceptance criterion $\sigma(I)/(I) = 0.5$. [b] Two crystals were used for data collection (see Experimental section). [c] Unit-cell parameters were averaged for the two data collections. [d] $R' = \Sigma[(F_o - F_c)w^{\frac{1}{2}}]/\Sigma(F_o w^{\frac{1}{2}})$, where $w = k/[\sigma^2(F) + |g|F^2]$.

from differences in the bonding interactions of the CuL, AgL, and AuL fragments with the prismatic dianion, even though all systems achieve substantially equivalent neutralization of the $Rh_6C(CO)_{15}$ unit, as can be inferred from a comparison of the CO stretching frequencies in Table 1. The hypothesis attributing σ- plus π-accepting ability to the CuL fragments and only σ-accepting ability to AgL and AuL fragments is in good agreement with the observed deformations of the Rh_6 prism upon co-ordination of these groups. The triangular faces show shrinkage effects, with respect to the parent dianion, only for the copper derivatives (see Table 2), indicating that some electron density has been removed from these faces *via* π interactions with the suitable copper *p* orbitals. Charge donation from the prismatic dianion *via* σ interactions, on the other hand, can explain the shortening of the inter-basal distances, as observed in all the derivatives, which is more marked in the silver and gold species. The latter effect may indicate that in the silver and gold species σ bonding makes up for the lack of π bonding in removing the charge excess from the Rh_6 unit and becomes stronger than in the copper derivatives.

Table 7. Fractional atomic co-ordinates for complex (**1**)

Atom	*x*	*y*	*z*
Rh(1)	0.632 65(5)	0.422 80(8)	0.334 28(4)
Rh(2)	0.556 61(5)	0.653 16(7)	0.334 32(5)
Rh(3)	0.479 40(5)	0.423 94(8)	0.334 37(4)
Ag	0.649 30(6)	0.500 04(10)	0.474 01(5)
C(0)	0.5	0.498 5(17)	0.25
C(1)	0.447 2(7)	0.616 4(11)	0.344 3(6)
O(1)	0.398 6(5)	0.672 6(8)	0.352 2(5)
C(2)	0.561 2(7)	0.270 0(10)	0.343 8(6)
O(2)	0.567 9(6)	0.159 4(8)	0.352 6(5)
C(3)	0.677 5(7)	0.615 2(11)	0.343 3(6)
O(3)	0.739 0(6)	0.668 2(8)	0.352 5(5)
C(4)	0.749 3(8)	0.356 3(12)	0.418 4(7)
O(4)	0.817 1(6)	0.310 5(11)	0.463 1(6)
C(5)	0.615 3(7)	0.778 3(12)	0.417 8(6)
O(5)	0.648 2(8)	0.858 6(10)	0.462 7(6)
C(6)	0.469 6(8)	0.365 6(11)	0.417 6(7)
O(6)	0.460 1(7)	0.330 1(11)	0.462 2(6)
C(7)	0.351 9(7)	0.351 9(11)	0.250 5(7)
O(7)	0.296 8(6)	0.297 6(11)	0.250 1(6)
C(8)	0.5	0.795 8(17)	0.25
O(8)	0.5	0.906 6(12)	0.25
N	0.734 6(7)	0.500 1(13)	0.602 7(6)
C(9)	0.780 0(8)	0.498 9(13)	0.669 7(8)
C(10)	0.836 8(9)	0.502 0(21)	0.756 2(7)
O(9)	0.5	0.0	0.0

Experimental

All operations were carried out under nitrogen; solvents were purified and stored under nitrogen. $K_2[Rh_6C(CO)_{15}]\cdot$*ca.*3thf,[8] $[PPh_4]_2[Rh_6C(CO)_{15}]$,[8] $[\{CuCl(PPh_3)\}_4]$,[9]

Table 8. Fractional atomic co-ordinates for complex (**2**)

Atom	*x*	*y*	*z*
Ag(1)	0.289 36(5)	0.123 05(4)	0.304 17(4)
Ag(2)	0.723 75(6)	0.362 71(4)	0.187 38(4)
Rh(1)	0.379 06(5)	0.296 53(4)	0.338 24(4)
Rh(2)	0.533 21(5)	0.153 55(4)	0.305 79(4)
Rh(3)	0.361 80(5)	0.153 76(4)	0.168 88(4)
Rh(4)	0.527 27(5)	0.239 97(4)	0.122 46(4)
Rh(5)	0.696 29(5)	0.241 33(4)	0.259 61(4)
Rh(6)	0.543 99(5)	0.385 31(4)	0.291 46(4)
P(1)	0.180 4(2)	0.047 8(1)	0.363 4(1)
P(2)	0.845 0(2)	0.436 9(1)	0.135 7(1)
C	0.506 0(5)	0.244 8(4)	0.247 8(4)
C(1)	0.258 3(8)	0.328 0(6)	0.414 0(6)
O(1)	0.187 6(8)	0.351 4(6)	0.458 1(6)
C(2)	0.544 1(7)	0.066 6(6)	0.353 2(6)
O(2)	0.559 3(6)	0.017 3(5)	0.381 3(6)
C(3)	0.223 8(9)	0.074 1(7)	0.108 8(6)
O(3)	0.142 0(7)	0.032 0(6)	0.069 8(5)
C(4)	0.571 9(7)	0.237 6(6)	0.014 9(6)
O(4)	0.598 0(7)	0.232 6(5)	−0.046 4(5)
C(5)	0.865 4(7)	0.244 5(6)	0.262 5(7)
O(5)	0.963 9(6)	0.241 1(7)	0.265 6(8)
C(6)	0.583 4(9)	0.507 6(6)	0.321 0(6)
O(6)	0.606 1(10)	0.579 8(5)	0.340 3(7)
C(7)	0.502 1(7)	0.267 9(5)	0.429 5(5)
O(7)	0.537 0(6)	0.292 9(4)	0.502 7(4)
C(8)	0.477 4(7)	0.051 2(6)	0.171 8(5)
O(8)	0.494 3(7)	−0.022 0(4)	0.129 1(4)
C(9)	0.253 8(7)	0.270 3(5)	0.223 1(6)
O(9)	0.170 0(5)	0.298 0(5)	0.200 2(4)
C(10)	0.664 6(8)	0.147 5(5)	0.121 8(5)
O(10)	0.702 7(6)	0.085 3(4)	0.072 8(4)
C(11)	0.699 4(8)	0.372 3(6)	0.372 7(6)
O(11)	0.764 3(6)	0.413 2(5)	0.434 6(4)
C(12)	0.445 8(7)	0.368 0(6)	0.166 9(6)
O(12)	0.389 6(7)	0.408 4(5)	0.136 8(5)
C(13)	0.424 5(7)	0.430 6(5)	0.379 8(5)
O(13)	0.396 5(6)	0.498 2(4)	0.430 6(4)
C(14)	0.713 5(7)	0.175 9(5)	0.340 2(5)
O(14)	0.788 2(5)	0.165 7(5)	0.388 9(4)
C(15)	0.371 9(8)	0.166 1(6)	0.053 7(5)
O(15)	0.313 9(6)	0.149 8(5)	−0.013 8(4)
C(17)	0.241 8(5)	−0.084 6(3)	0.424 2(3)
C(18)	0.294 0(5)	−0.165 0(3)	0.416 6(3)
C(19)	0.355 3(5)	−0.214 2(3)	0.345 6(3)
C(20)	0.364 5(5)	−0.183 1(3)	0.282 1(3)
C(21)	0.312 3(5)	−0.102 7(3)	0.289 7(3)
C(16)	0.250 9(5)	−0.053 5(3)	0.360 7(3)
C(23)	0.073 7(4)	0.165 3(4)	0.511 3(4)
C(24)	0.078 4(4)	0.231 8(4)	0.598 9(4)
C(25)	0.187 0(4)	0.257 4(4)	0.655 6(4)
C(26)	0.290 9(4)	0.216 6(4)	0.624 7(4)
C(27)	0.286 1(4)	0.150 1(4)	0.537 1(4)
C(22)	0.177 5(4)	0.124 5(4)	0.480 4(4)
C(29)	−0.042 7(4)	−0.032 7(4)	0.344 3(3)
C(30)	−0.157 5(4)	−0.063 9(4)	0.300 1(3)
C(31)	−0.201 9(4)	−0.051 8(4)	0.224 4(3)
C(32)	−0.131 5(4)	−0.008 7(4)	0.192 8(3)
C(33)	−0.016 7(4)	0.022 4(4)	0.237 0(3)
C(28)	0.027 7(4)	0.010 4(4)	0.312 7(3)
C(35)	0.976 1(5)	0.518 0(5)	0.301 6(4)
C(36)	1.075 8(5)	0.561 0(5)	0.364 3(4)
C(37)	1.179 9(5)	0.572 8(5)	0.336 1(4)
C(38)	1.184 4(5)	0.541 5(5)	0.245 3(4)
C(39)	1.084 7(5)	0.498 5(5)	0.182 6(4)
C(34)	0.980 6(5)	0.486 8(5)	0.210 8(4)
C(41)	0.650 5(5)	0.534 9(4)	0.114 5(4)
C(42)	0.593 1(5)	0.605 4(4)	0.101 8(4)
C(43)	0.658 0(5)	0.667 4(4)	0.088 9(4)
C(44)	0.780 2(5)	0.658 8(4)	0.088 6(4)
C(45)	0.837 5(5)	0.588 2(4)	0.101 2(4)
C(40)	0.772 7(5)	0.526 3(4)	0.114 2(4)
C(47)	0.860 2(5)	0.364 1(4)	−0.049 7(4)
C(48)	0.889 6(5)	0.296 1(4)	−0.128 8(4)
C(49)	0.948 9(5)	0.220 9(4)	−0.127 9(4)
C(50)	0.978 7(5)	0.213 8(4)	−0.047 9(4)
C(51)	0.949 2(5)	0.281 8(4)	0.031 1(4)
C(46)	0.890 0(5)	0.356 9(4)	0.030 2(4)

Table 9. Fractional atomic co-ordinates for complex (**3**)

Atom	*x*	*y*	*z*
Cu(1)	0.299 69(7)	0.120 66(5)	0.304 25(5)
Cu(2)	0.707 86(7)	0.364 75(5)	0.187 63(5)
Rh(1)	0.376 79(4)	0.291 56(3)	0.336 75(3)
Rh(2)	0.531 18(4)	0.151 01(3)	0.309 56(3)
Rh(3)	0.364 98(4)	0.147 19(3)	0.171 12(3)
Rh(4)	0.526 74(4)	0.242 86(3)	0.123 36(3)
Rh(5)	0.692 26(4)	0.245 81(3)	0.260 49(3)
Rh(6)	0.540 91(4)	0.387 69(3)	0.288 99(3)
P(1)	0.191 22(14)	0.048 74(11)	0.358 12(11)
P(2)	0.828 77(14)	0.435 11(11)	0.141 71(11)
C	0.504 4(4)	0.244 4(3)	0.248 5(3)
C(1)	0.256 3(6)	0.321 0(4)	0.411 9(5)
O(1)	0.185 3(5)	0.342 2(4)	0.455 9(4)
C(2)	0.541 0(6)	0.063 9(4)	0.361 1(4)
O(2)	0.554 5(5)	0.013 6(4)	0.392 5(4)
C(3)	0.233 5(7)	0.062 0(5)	0.110 9(5)
O(3)	0.155 5(5)	0.012 7(4)	0.070 6(4)
C(4)	0.572 3(5)	0.246 5(4)	0.019 2(4)
O(4)	0.600 4(4)	0.243 0(4)	−0.044 8(3)
C(5)	0.858 4(6)	0.254 9(5)	0.264 7(5)
O(5)	0.958 4(4)	0.258 9(4)	0.271 1(5)
C(6)	0.581 6(7)	0.513 2(5)	0.316 5(5)
O(6)	0.599 1(7)	0.588 1(3)	0.333 6(4)
C(7)	0.499 9(5)	0.265 8(4)	0.430 2(4)
O(7)	0.529 2(5)	0.290 5(3)	0.503 3(3)
C(8)	0.480 5(5)	0.046 1(4)	0.178 0(4)
O(8)	0.496 9(5)	−0.029 8(3)	0.137 6(3)
C(9)	0.254 7(5)	0.262 0(4)	0.221 4(4)
O(9)	0.170 9(4)	0.285 9(4)	0.194 9(3)
C(10)	0.663 5(5)	0.152 0(4)	0.124 5(4)
O(10)	0.701 5(4)	0.089 0(3)	0.075 2(3)
C(11)	0.693 0(6)	0.377 0(4)	0.370 3(4)
O(11)	0.757 6(4)	0.420 0(3)	0.432 3(3)
C(12)	0.440 9(6)	0.369 3(4)	0.165 6(4)
O(12)	0.382 8(4)	0.410 6(3)	0.135 1(3)
C(13)	0.420 9(5)	0.429 3(4)	0.378 1(4)
O(13)	0.394 3(4)	0.497 9(3)	0.428 8(3)
C(14)	0.712 4(6)	0.175 9(4)	0.341 6(4)
O(14)	0.787 0(4)	0.163 6(3)	0.388 3(3)
C(15)	0.375 3(6)	0.162 8(4)	0.054 6(4)
O(15)	0.318 4(4)	0.142 7(4)	−0.128 8(3)
C(17)	0.837 2(3)	0.594 5(3)	0.110 2(3)
C(18)	0.785 9(3)	0.667 3(3)	0.095 7(3)
C(19)	0.664 2(3)	0.675 1(3)	0.091 0(3)
C(20)	0.593 9(3)	0.610 2(3)	0.100 9(3)
C(21)	0.645 3(3)	0.537 5(3)	0.115 4(3)
C(16)	0.766 9(3)	0.529 6(3)	0.120 0(3)
C(23)	0.851 3(4)	0.367 1(3)	−0.040 3(3)
C(24)	0.881 3(4)	0.299 7(3)	−0.118 4(3)
C(25)	0.937 1(4)	0.222 5(3)	−0.116 8(3)
C(26)	0.962 8(4)	0.212 9(3)	−0.037 0(3)
C(27)	0.932 7(4)	0.280 3(3)	0.041 2(3)
C(22)	0.877 0(4)	0.357 4(3)	0.039 5(3)
C(29)	1.070 0(4)	0.493 7(3)	0.193 8(2)
C(30)	1.167 8(4)	0.535 4(3)	0.257 9(2)
C(31)	1.157 9(4)	0.567 2(3)	0.347 9(2)
C(32)	1.050 2(4)	0.557 3(3)	0.373 8(2)
C(33)	0.952 4(4)	0.515 5(3)	0.309 8(2)
C(28)	0.962 3(4)	0.483 7(3)	0.219 8(2)
C(35)	−0.002 0(4)	0.032 8(3)	0.233 2(3)
C(36)	−0.116 2(4)	0.002 9(3)	0.188 9(3)
C(37)	−0.188 0(4)	−0.046 2(3)	0.217 4(3)
C(38)	−0.145 7(4)	−0.065 4(3)	0.290 1(3)
C(39)	−0.031 5(4)	−0.035 4(3)	0.334 4(3)
C(34)	0.040 4(4)	0.013 6(3)	0.305 9(3)
C(41)	0.243 0(4)	−0.090 8(3)	0.419 0(2)
C(42)	0.291 8(4)	−0.173 2(3)	0.411 7(2)
C(43)	0.352 0(4)	−0.222 0(3)	0.340 6(2)
C(44)	0.363 2(4)	−0.188 4(3)	0.276 9(2)
C(45)	0.314 4(4)	−0.106 0(3)	0.284 2(2)
C(40)	0.254 2(4)	−0.057 2(3)	0.355 2(2)
C(47)	0.081 7(3)	0.161 4(3)	0.502 2(3)
C(48)	0.083 3(3)	0.226 2(3)	0.589 4(3)
C(49)	0.188 5(3)	0.250 6(3)	0.648 3(3)
C(50)	0.292 2(3)	0.210 2(3)	0.620 1(3)
C(51)	0.290 6(3)	0.145 4(3)	0.532 9(3)
C(46)	0.185 4(3)	0.121 1(3)	0.474 0(3)

$[\{AgCl(PPh_3)\}_4]$,[10] and $[AuCl(PPh_3)]$[11] were prepared according to the literature.

Preparations.—$[Rh_6C(CO)_{15}\{Ag(NCMe)\}_2]$.0.5MeCN. Due to the particular light-sensitivity of the product, manipulations are best performed in dim light. A solution of $K_2[Rh_6C(CO)_{15}]$·*ca.*3thf (284.4 mg, 0.212 mmol in 3 cm^3 MeOH) was added under stirring to a solution of $AgBF_4$ (81.3 mg, 0.418 mmol) in MeOH–MeCN (1:1) (3 cm^3). The fine yellow precipitate immediately formed was separated from the brown mother-liquor by filtration, washed with MeOH (5 cm^3), and vacuum dried. Recrystallization was performed by extracting the product with thf–MeCN (9:1, 15 cm^3) then cautiously layering n-hexane (40 cm^3) on the resulting brown-yellow solution and leaving in the dark. When the slow diffusion of the solvents was complete, the product, as a yellow powder, was separated from the mother-liquor, vacuum dried, and stored in the dark. Yield: 125 mg, 45%. Analysis revealed the presence of 0.5 mol of MeCN (Found: C, 18.65; H, 0.50; N, 2.65. Calc. for $C_{21}H_{7.5}Ag_2N_{2.5}O_{15}Rh_6$: C, 18.45; H, 0.55; N, 2.55%).

$[Rh_6C(CO)_{15}\{Ag(NCMe)\}_2]$·0.5MeOH *for* X-*ray diffraction.* The following procedure was used to obtain crystals containing clathrated MeOH isomorphous to the previously reported copper analogue.[3] A solution of $K_2[Rh_6C(CO)_{15}]$·*ca.* 3 thf (234 mg, 0.174 mmol in 4 cm^3 of a 10:1 mixture of MeOH and MeCN) was carefully layered with a solution of $AgBF_4$ (134 mg, 0.688 mol, in 9 cm^3 of the same solvent mixture). When the slow diffusion was complete, the amber-yellow crystals containing solvated MeOH were recovered as above.

$[Rh_6C(CO)_{15}\{Ag(PPh_3)\}_2]$. A solution of $K_2[Rh_6C(CO)_{15}]$·*ca.* 3 thf (271.5 mg, 0.202 mmol in 5 cm^3 MeOH) was added to a suspension of $[\{AgCl(PPh_3)\}_4]$ (210.4 mg, 0.13 mmol in 2 cm^3 $CHCl_3$). After stirring for 1 h, the amber-yellow flakes precipitated were filtered off from the brown mother-liquor, washed with MeOH (5 cm^3, four times), and vacuum dried. Recrystallization was performed by extraction with thf (6 cm^3) and cautious layering of n-hexane (18 cm^3) on the resulting solution. When the slow diffusion was complete, the product, as amber-yellow crystals, was separated from the mother-liquor, washed carefully by decantation with n-hexane, and vacuum dried. The product, fairly air stable, darkened after a few days, but was still soluble in thf with the expected i.r. spectrum. Yield: 230 mg, 60% (Found: C, 35.1; H, 2.00. Calc. for $C_{52}H_{30}Ag_2O_{15}P_2Rh_6$: C, 34.9; H, 1.70%).

$[Rh_6C(CO)_{15}\{Cu(PPh_3)\}_2]$. A solution of $K_2[Rh_6C(CO)_{15}]$·*ca.* 3 thf (271.5 mg, 0.202 mmol in 5 cm^3 MeOH) was added to a suspension of $[\{CuCl(PPh_3)\}_4]$ (182.2 mg, 0.126 mmol in 2 cm^3 $CHCl_3$). After stirring for 1 h, the fine yellow precipitate was filtered from the brown mother-liquor, washed with MeOH (5 cm^3, four times), and vacuum dried. Recrystallization was by extraction with thf (20 cm^3) and cautious layering of n-hexane (40 cm^3) on the resulting solution. When the slow diffusion was

Table 10. Fractional atomic co-ordinates for complex (**4**)

Atom	*x*	*y*	*z*
Au(1)	0.193 15(6)	−0.100 84(9)	0.351 82(5)
Rh(1)	0.178 67(10)	−0.175 03(15)	0.421 76(8)
Rh(2)	0.089 41(10)	−0.193 27(16)	0.364 09(8)
Rh(3)	0.193 69(11)	−0.290 80(16)	0.364 16(8)
Rh(4)	0.145 59(11)	−0.436 88(15)	0.399 93(9)
Rh(5)	0.132 25(10)	−0.323 37(16)	0.458 12(8)
Rh(6)	0.042 01(10)	−0.338 39(16)	0.401 05(9)
P(1)	0.225 9(4)	0.003 9(5)	0.313 3(3)
Au(2)	0.305 96(6)	0.410 87(10)	0.169 17(5)
Rh(7)	0.284 66(10)	0.354 38(16)	0.097 24(8)
Rh(8)	0.307 19(10)	0.222 50(16)	0.151 12(8)
Rh(9)	0.397 06(10)	0.331 25(17)	0.133 49(9)
Rh(10)	0.419 77(11)	0.201 48(21)	0.080 32(10)
Rh(11)	0.307 00(11)	0.226 66(19)	0.044 12(9)
Rh(12)	0.329 24(11)	0.093 35(16)	0.098 58(9)
P(2)	0.284 5(4)	0.502 3(6)	0.214 9(3)
P(3)	0.963 9(3)	−0.804 1(5)	0.401 0(3)
P(4)	0.489 3(3)	−0.760 2(6)	0.409 9(3)
C(01)	0.128 0(10)	−0.296 1(16)	0.401 0(8)
C(1)	0.218 9(17)	−0.071 3(18)	0.439 0(12)
O(1)	0.235 2(11)	0.002 5(13)	0.450 9(8)
C(2)	0.058 1(16)	−0.102 7(20)	0.332 9(10)
O(2)	0.034 5(11)	−0.044 4(15)	0.313 7(7)
C(3)	0.250 5(14)	−0.282 1(27)	0.333 7(9)
O(3)	0.280 6(12)	−0.274 1(22)	0.309 6(7)
C(4)	0.147 5(18)	−0.561 6(11)	0.404 7(12)
O(4)	0.138 5(11)	−0.642 8(10)	0.401 1(7)
C(5)	−0.027 6(10)	−0.390 6(23)	0.408 3(11)
O(5)	−0.073 5(8)	−0.417 4(18)	0.416 4(8)
C(6)	0.117 5(11)	−0.381 9(18)	0.499 9(6)
O(6)	0.108 7(10)	−0.421 1(15)	0.527 2(5)
C(7)	0.097 0(13)	−0.108 7(21)	0.408 7(9)
O(7)	0.074 8(10)	−0.046 6(17)	0.423 2(7)
C(8)	0.209 7(14)	−0.423 5(22)	0.367 2(10)
O(8)	0.245 6(9)	−0.477 8(15)	0.359 2(7)
C(9)	0.252 3(16)	−0.248 2(24)	0.408 7(11)
O(9)	0.302 2(10)	−0.258 2(15)	0.421 8(7)
C(10)	0.123 4(14)	−0.278 5(22)	0.328 8(12)
O(10)	0.108 7(10)	−0.293 1(16)	0.296 8(8)
C(11)	0.173 5(11)	−0.212 2(18)	0.477 5(9)
O(11)	0.191 1(11)	−0.173 4(18)	0.504 8(8)
C(12)	0.007 1(13)	−0.258 3(20)	0.359 4(9)
O(12)	−0.037 3(10)	−0.242 6(16)	0.342 6(7)
C(13)	0.046 3(13)	−0.273 1(20)	0.451 1(9)
O(13)	0.016 6(9)	−0.230 9(13)	0.468 5(6)
C(14)	0.196 2(15)	−0.420 5(24)	0.449 3(11)
O(14)	0.237 9(10)	−0.452 3(15)	0.469 6(7)
C(15)	0.065 1(15)	−0.444 3(24)	0.370 5(11)
O(15)	0.039 7(11)	−0.496 5(17)	0.345 7(8)
C(02)	0.341 3(12)	0.240 2(19)	0.098 1(9)
C(16)	0.286 5(15)	0.219 4(24)	0.197 0(6)
O(16)	0.269 5(13)	0.227 2(22)	0.226 3(5)
C(17)	0.242 3(11)	0.460 5(13)	0.094 6(9)
O(17)	0.217 0(10)	0.531 4(12)	0.098 9(8)
C(18)	0.435 1(14)	0.411 5(19)	0.166 5(9)
O(18)	0.463 9(11)	0.470 9(15)	0.182 7(7)
C(19)	0.327 7(16)	−0.292 2(11)	0.089 7(11)
O(19)	0.329 4(13)	−0.111 2(10)	0.087 6(8)
C(20)	0.284 5(14)	0.209 5(23)	−0.004 6(5)
O(20)	0.263 6(14)	0.178 9(21)	−0.034 4(5)
C(21)	0.482 1(12)	0.154 7(24)	0.060 8(9)
O(21)	0.510 3(11)	0.112 6(18)	0.040 0(7)
C(22)	0.416 0(19)	0.087 9(30)	0.111 4(13)
O(22)	0.451 8(12)	0.031 5(19)	0.128 0(8)
C(23)	0.467 2(20)	0.283 6(29)	0.111 8(13)
O(23)	0.522 8(14)	0.294 2(21)	0.119 0(9)
C(24)	0.254 7(14)	0.120 5(22)	0.058 0(10)
O(24)	0.210 9(11)	0.084 0(16)	0.050 9(8)
C(25)	0.226 7(15)	0.265 7(23)	0.122 4(10)
O(25)	0.176 6(10)	0.252 4(15)	0.120 6(6)
C(26)	0.261 2(16)	0.346 0(24)	0.044 8(11)
C(113)	0.231 8(9)	0.218 7(12)	0.382 7(6)
C(114)	0.269 1(9)	0.282 2(12)	0.369 4(6)
C(115)	0.294 7(9)	0.262 4(12)	0.337 9(6)
C(116)	0.283 2(9)	0.179 0(12)	0.319 8(6)
C(121)	0.293 1(7)	−0.032 3(13)	0.296 0(7)
C(122)	0.300 1(7)	−0.019 5(13)	0.259 2(7)
C(123)	0.353 0(7)	−0.042 7(13)	0.246 8(7)
C(124)	0.398 9(7)	−0.078 8(13)	0.271 2(7)
C(125)	0.391 8(7)	−0.091 7(13)	0.308 0(7)
C(126)	0.338 9)7)	−0.063 4(13)	0.320 4(7)
C(131)	0.173 8(9)	0.021 6(17)	0.272 8(5)
C(132)	0.168 7(9)	0.107 5(17)	0.255 9(5)
C(133)	0.128 5(9)	0.120 8(17)	0.224 5(5)
C(134)	0.093 5(9)	0.048 1(17)	0.209 8(5)
C(135)	0.098 7(9)	−0.037 8(17)	0.226 7(5)
C(136)	0.138 8(9)	−0.051 0(17)	0.258 1(5)
C(211)	0.221 2(9)	0.456 7(16)	0.236 5(9)
C(212)	0.217 8(9)	0.458 2(16)	0.274 2(9)
C(213)	0.165 9(9)	0.432 4(16)	0.287 3(9)
C(214)	0.117 6(9)	0.405 0(16)	0.262 7(9)
C(215)	0.121 1(9)	0.403 5(16)	0.225 1(9)
C(216)	0.172 9(9)	0.429 3(16)	0.212 0(9)
C(221)	0.343 5(9)	0.507 0(17)	0.250 3(6)
C(222)	0.360 9(9)	0.591 1(17)	0.266 3(6)
C(223)	0.411 1(9)	0.596 4(17)	0.291 9(6)
C(224)	0.443 9(9)	0.517 7(17)	0.301 7(6)
C(225)	0.426 5(9)	0.433 6(17)	0.285 6(6)
C(226)	0.376 3(9)	0.428 2(17)	0.260 0(6)
C(231)	0.264 0(10)	0.619 5(12)	0.203 1(7)
C(232)	0.225 3(10)	0.670 5(12)	0.221 2(7)
C(233)	0.215 7(10)	0.763 0(12)	0.212 7(7)
C(234)	0.244 8(10)	0.604 4(12)	0.186 1(7)
C(235)	0.283 5(10)	0.753 5(12)	0.167 9(7)
C(236)	0.293 0(10)	0.661 0(12)	0.176 4(7)
C(311)	0.944 8(8)	−0.914 5(11)	0.416 5(7)
C(312)	0.939 9(8)	−0.925 7(11)	0.453 7(7)
C(313)	0.924 2(8)	−1.010 7(11)	0.466 8(7)
C(314)	0.913 4(8)	−1.084 5(11)	0.442 7(7)
C(315)	0.918 3(8)	−1.073 3(11)	0.405 5(7)
C(316)	0.934 0(8)	−0.988 3(11)	0.392 4(7)
C(321)	1.018 4(8)	−0.760 0(14)	0.433 1(5)
C(322)	1.066 3(8)	−0.814 6(14)	0.446 4(5)
C(323)	1.110 4(8)	−0.779 5(14)	0.472 3(5)
C(324)	1.106 6(8)	−0.689 8(14)	0.485 0(5)
C(325)	1.058 8(8)	−0.635 2(14)	0.471 7(5)
C(326)	1.014 6(8)	−0.670 2(14)	0.445 7(5)
C(331)	0.900 3(7)	−0.731 1(13)	0.397 0(6)
C(332)	0.903 7(7)	−0.648 3(13)	0.378 3(6)
C(333)	0.858 0(7)	−0.585 1(13)	0.377 0(6)
C(334)	0.808 9(7)	−0.604 6(13)	0.394 3(6)
C(335)	0.805 6(7)	−0.687 3(13)	0.412 9(6)
C(336)	0.851 3(7)	−0.750 6(13)	0.414 3(6)
C(341)	0.985 2(10)	−0.813 5(14)	0.356 2(6)
C(342)	1.044 2(10)	−0.804 0(14)	0.351 9(6)
C(343)	1.061 5(10)	−0.808 1(14)	0.316 9(6)
C(344)	1.019 7(10)	−0.821 8(14)	0.286 2(6)
C(345)	0.960 7(10)	−0.831 3(14)	0.290 5(6)
C(346)	0.943 4(10)	−0.827 2(14)	0.325 5(6)
C(411)	0.559 6(8)	−0.746 9(19)	0.437 9(7)
C(412)	0.605 3(8)	−0.806 8(19)	0.433 3(7)
C(413)	0.658 1(8)	−0.801 8(19)	0.456 8(7)
C(414)	0.665 1(8)	−0.736 8(19)	0.484 9(7)
C(415)	0.619 3(8)	−0.676 8(19)	0.489 5(7)
C(416)	0.566 6(8)	−0.681 9(19)	0.466 0(7)
C(421)	0.452 5(11)	−0.858 7(14)	0.423 8(7)
C(422)	0.391 9(11)	−0.867 6(14)	0.415 3(7)
C(423)	0.364 7(11)	−0.950 3(14)	0.422 0(7)
C(424)	0.398 1(11)	−1.024 0(14)	0.437 2(7)
C(425)	0.458 7(11)	−1.015 1(14)	0.445 7(7)
C(426)	0.485 9(11)	−0.932 4(14)	0.439 1(7)
C(431)	0.501 0(11)	−0.772 5(17)	0.363 6(6)

Table 10 (*continued*)

Atom	*x*	*y*	*z*	Atom	*x*	*y*	*z*
O(26)	0.227 0(13)	0.374 1(18)	0.020 8(9)	C(432)	0.465 5(11)	−0.828 7(17)	0.339 2(6)
C(27)	0.394 6(14)	0.233 0(22)	0.175 1(10)	C(433)	0.474 1(11)	−0.832 5(17)	0.302 3(6)
O(27)	0.424 2(12)	0.206 9(18)	0.199 4(8)	C(434)	0.518 2(11)	−0.780 1(17)	0.289 8(6)
C(28)	0.363 3(13)	0.420 2(23)	0.095 5(10)	C(435)	0.553 7(11)	−0.723 9(17)	0.314 2(6)
O(28)	0.376 6(11)	0.489 0(19)	0.078 2(8)	C(436)	0.545 1(11)	−0.720 1(17)	0.351 0(6)
C(29)	0.304 5(16)	0.083 9(25)	0.147 4(12)	C(441)	0.442 0(9)	−0.664 6(12)	0.415 9(9)
O(29)	0.278 1(13)	0.030 3(21)	0.165 0(9)	C(442)	0.420 3(9)	−0.653 0(12)	0.449 4(9)
C(30)	0.388 7(20)	0.269 7(33)	0.037 1(14)	C(443)	0.385 6(9)	−0.577 1(12)	0.454 8(9)
O(30)	0.403 8(14)	0.326 3(22)	0.013 0(9)	C(444)	0.372 5(9)	−0.512 8(12)	0.426 8(9)
C(111)	0.245 9(9)	0.115 4(12)	0.333 2(6)	C(445)	0.394 1(9)	−0.524 4(12)	0.393 4(9)
C(112)	0.220 3(9)	0.135 2(12)	0.364 7(6)	C(446)	0.428 8(9)	−0.600 3(12)	0.387 9(9)

Table 11. Fractional atomic co-ordinates for complex (**5**)

Atom	*x*	*y*	*z*	Atom	*x*	*y*	*z*
Au(1)	0.290 49(4)	0.118 93(4)	0.304 60(4)	C(15)	0.371 1(12)	0.165 8(9)	0.053 8(9)
Au(2)	0.719 45(5)	0.365 92(4)	0.184 91(4)	O(15)	0.312 0(9)	0.146 0(8)	−0.012 8(7)
Rh(1)	0.378 90(8)	0.294 84(6)	0.337 83(7)	C(17)	0.076 8(6)	0.165 7(6)	0.509 2(6)
Rh(2)	0.533 92(8)	0.152 50(6)	0.306 13(7)	C(18)	0.081 2(6)	0.231 4(6)	0.597 0(6)
Rh(3)	0.361 99(8)	0.151 40(6)	0.169 48(7)	C(19)	0.188 9(6)	0.256 2(6)	0.654 4(6)
Rh(4)	0.524 66(8)	0.240 47(6)	0.121 92(6)	C(20)	0.292 2(6)	0.215 2(6)	0.624 1(6)
Rh(5)	0.694 16(8)	0.243 27(6)	0.258 81(7)	C(21)	0.287 8(6)	0.149 4(6)	0.536 3(6)
Rh(6)	0.541 69(8)	0.386 18(6)	0.290 10(7)	C(16)	0.180 1(6)	0.124 7(6)	0.478 8(6)
P(1)	0.185 2(3)	0.048 9(2)	0.363 4(2)	C(23)	0.243 2(7)	−0.085 2(5)	0.423 7(5)
P(2)	0.840 4(3)	0.435 9(2)	0.136 4(2)	C(24)	0.293 4(7)	−0.166 5(5)	0.416 7(5)
C	0.507 5(10)	0.245 5(7)	0.249 3(8)	C(25)	0.353 9(7)	−0.216 5(5)	0.345 7(5)
C(1)	0.260 0(11)	0.326 6(9)	0.412 7(10)	C(26)	0.364 3(7)	−0.185 2(5)	0.281 8(5)
O(1)	0.191 7(10)	0.347 8(8)	0.459 9(8)	C(27)	0.314 1(7)	−0.104 0(5)	0.288 8(5)
C(2)	0.548 0(12)	0.065 3(9)	0.355 1(9)	C(22)	0.253 6(7)	−0.053 9(5)	0.359 8(5)
O(2)	0.560 5(9)	0.013 6(8)	0.383 8(9)	C(29)	−0.037 7(7)	−0.031 3(6)	0.341 9(5)
C(3)	0.225 4(12)	0.070 7(10)	0.107 9(10)	C(30)	−0.151 9(7)	−0.062 8(6)	0.297 1(5)
O(3)	0.145 5(10)	0.026 2(9)	0.070 0(7)	C(31)	−0.195 3(7)	−0.049 5(6)	0.221 6(5)
C(4)	0.566 3(12)	0.239 4(9)	0.015 4(9)	C(32)	−0.124 5(7)	−0.004 7(6)	0.190 9(5)
O(4)	0.595 4(9)	0.233 7(7)	−0.048 1(7)	C(33)	−0.010 2(7)	0.026 8(6)	0.235 6(5)
C(5)	0.861 0(13)	0.248 2(9)	0.261 3(10)	C(28)	0.033 2(7)	0.013 5(6)	0.311 1(5)
O(5)	0.960 6(9)	0.246 6(9)	0.266 9(10)	C(35)	1.080 8(8)	0.496 5(7)	0.185 5(5)
C(6)	0.578 1(15)	0.509 2(11)	0.319 5(10)	C(36)	1.179 7(8)	0.539 6(7)	0.249 1(5)
O(6)	0.597 1(12)	0.584 3(8)	0.339 2(9)	C(37)	1.173 3(8)	0.571 0(7)	0.339 7(5)
C(7)	0.504 2(11)	0.268 1(9)	0.426 6(10)	C(38)	1.068 1(8)	0.559 3(7)	0.366 8(5)
O(7)	0.538 4(9)	0.292 6(7)	0.502 3(7)	C(39)	0.969 2(8)	0.516 2(7)	0.303 3(5)
C(8)	0.481 2(11)	0.049 0(10)	0.172 1(9)	C(34)	0.975 6(8)	0.484 8(7)	0.212 6(5)
O(8)	0.496 5(9)	−0.026 3(7)	0.130 8(7)	C(41)	0.839 5(6)	0.589 4(6)	0.102 9(6)
C(9)	0.255 4(12)	0.268 8(9)	0.222 9(9)	C(42)	0.785 4(6)	0.660 5(6)	0.088 6(6)
O(9)	0.171 0(8)	0.294 6(7)	0.197 2(7)	C(43)	0.663 5(6)	0.669 7(6)	0.086 8(6)
C(10)	0.659 7(10)	0.149 2(9)	0.123 3(9)	C(44)	0.595 8(6)	0.607 6(6)	0.099 3(6)
O(10)	0.700 2(9)	0.084 6(7)	0.071 5(7)	C(45)	0.650 0(6)	0.536 5(6)	0.113 6(6)
C(11)	0.694 9(10)	0.372 3(9)	0.371 1(9)	C(40)	0.771 8(6)	0.527 4(6)	0.115 4(6)
O(11)	0.760 6(8)	0.414 5(7)	0.432 7(6)	C(47)	0.855 5(8)	0.364 0(5)	−0.046 3(7)
C(12)	0.440 4(14)	0.368 0(10)	0.168 0(10)	C(48)	0.884 9(8)	0.296 3(5)	−0.125 4(7)
O(12)	0.384 3(10)	0.409 0(7)	0.135 0(7)	C(49)	0.943 2(8)	0.220 4(5)	−0.124 7(7)
C(13)	0.423 5(11)	0.430 6(9)	0.381 5(9)	C(50)	0.972 1(8)	0.212 1(5)	−0.044 9(7)
O(13)	0.394 4(8)	0.498 6(6)	0.429 8(7)	C(51)	0.942 6(8)	0.279 8(5)	0.034 1(7)
C(14)	0.715 4(12)	0.176 8(9)	0.339 6(10)	C(46)	0.884 4(8)	0.355 7(5)	0.033 4(7)
O(14)	0.789 1(8)	0.165 1(7)	0.387 5(7)				

complete, the yellow crystals were separated from the mother-liquor, washed carefully by decantation with n-hexane, and vacuum dried. The crystalline product was air stable for several days. Yield: 250 mg, 70% (Found: C, 36.55; H, 1.95. Calc. for $C_{52}H_{30}Cu_2O_{15}P_2Rh_6$: C, 36.7; H, 1.80%).

$[Rh_6C(CO)_{15}\{Au(PPh_3)\}_2]$. A solution of $K_2[Rh_6C(CO)_{15}]\cdot$ *ca.* 3 thf (357 mg, 0.266 mmol in 3 cm^3 MeOH) was added to a suspension in $CHCl_3$ (1 cm^3) of $[AuCl(PPh_3)]$ (263 mg, 0.533 mmol), while stirring. A fine lemon-yellow precipitate was quickly formed. The product was filtered off from the mother-liquor, washed with MeOH (2 cm^3, three times), and vacuum dried. The product obtained in nearly quantitative yield was generally of good purity; however, when crystalline specimens were desired, recrystallization was performed after extraction with thf (40 cm^3) by cautious layering of n-hexane (80 cm^3) on the resulting solution and leaving in the dark. When the diffusion of the liquid phase was complete the golden-yellow crystals suitable for *X*-ray diffraction were washed with n-hexane and vacuum dried. The crystals were fairly air stable and though showing some darkening after a few days they were still soluble in thf and exhibited the expected i.r. spectrum. Yield: 400 mg, 75% (Found: C, 31.7; H, 1.45. Calc. for $C_{52}H_{30}Au_2O_{15}P_2Rh_6$: C, 31.75; H, 1.55%).

$[PPh_4][Rh_6C(CO)_{15}\{Au(PPh_3)\}]$. The salt $[PPh_4]_2[Rh_6C(CO)_{15}]$ (213 mg, 0.123 mmol) and $[Rh_6C(CO)_{15}\{Au(PPh_3)\}_2]$ (237 mg, 0.121 mmol) were treated with thf (5 cm^3) and the mixture stirred at room temperature. I.r. monitoring of the clear orange-yellow solution showed that equilibration to give the monoanion was complete after about 1 h. Propan-2-ol (50 cm^3) was added to induce precipitation, which was completed by concentration in vacuum to about 40 cm^3. The yellow precipitate was separated from the mother-liquor by filtration, washed with propan-2-ol (5 + 5 cm^3), and vacuum dried. Yield: 360 mg, 80% (Found: C, 37.6; H, 1.75. Calc. for $C_{58}H_{35}AuO_{15}P_2Rh_6$: C, 37.7; H, 1.90%). The product obtained was of good purity; however, in order to prepare good crystals, recrystallization with the slow-diffusion technique was performed by dissolution in the minimum amount of thf and cautious layering of methanol–propan-2-ol (1:9).

Crystallography.—Crystal data and details of the measurements for all complexes are reported in Table 6. The diffraction experiments were carried out on an Enraf-Nonius CAD4 diffractometer equipped with Mo-K_α radiation, at room temperature. The unit-cell parameters were determined by least-squares refinement of the setting angles of 25 well centred high θ reflections. Diffraction intensities were corrected for Lorentz and polarization factors. Absorption correction for (**1**)—(**3**) and (**5**) was applied by the Walker and Stuart method,[12] once the complete structural models were known and all atoms refined isotropically. For complex (**1**) advantage was taken of the isomorphism with crystals of $[Rh_6C(CO)_{15}\{Cu(NCMe)\}_2]$ (**6**); a first attempt to refine all metal atom positions taken from the latter was successful. Subsequent Fourier-difference maps afforded the positions of all light atoms. As previously observed for crystals of (**6**), a residual peak of *ca.* 1.3 e Å^{-3} was found around an inversion centre (0, $\frac{1}{2}$, 0). It was attributed in a similar manner to a small fraction of a disordered methanol molecule; the occupancy of the supposed oxygen atoms refined to 0.24.

The structure of complex (**2**) was solved by the Patterson method which afforded the positions of a metal triangle. The remaining heavy atoms and the light atoms were located by subsequent Fourier and Fourier-difference maps. Crystals of (**3**) and (**5**) were found to be isomorphous with those of (**2**) so that the co-ordinates from the latter could be used as preliminary input in the refinement of both (**3**) and (**5**).

Crystals of complex (**4**) proved to be unstable to *X*-rays. A first data collection had to be terminated after measurement of 4 430 reflections in the range 3 < θ < 20° because decay of the reference reflections exceeded 40% of their initial values. The data collection was continued on a new crystal and 5 140 more reflections were collected within the same θ range. Care was taken in order to use the same 25 reflections for cell refinement as well as the reference reflections during data collection, for scaling purposes. The two data sets were then scaled and merged, affording a total of 9 570 measured reflections.

Crystals of (**5**) were well behaved, although partial decay (*ca.* 20%) prevented extension of the data collection beyond $\theta_{max.} = 23°$.

The structure of (**4**) proved difficult to solve because of the presence of two independent molecules in the unit cell, as indicated by density calculations. After several attempts by conventional Patterson and direct methods, the structure was solved by using the SHELX 86[13a] package which showed the positions of two independent metal-atom polyhedra. Due to the poor quality of data, geometrical constraints were used for terminal CO groups during the initial refinement cycles. While in (**4**) only the heavy atoms (Au, Rh, and P) could be treated anisotropically, full anisotropy was used for complexes (**1**)—(**3**) and (**5**). A rigid-body model was also applied (C–C–C 120°, C–C 1.395 Å) to the phenyl-ring carbon atoms in (**2**), (**3**), and (**5**). Hydrogen atoms for the methyl group in (**1**) and for the phenyl rings in (**2**), (**3**), and (**5**) were added in calculated positions and not refined (C–H 1.08 Å), though their contribution to the structural models was taken into account. For (**1**) approximate H-atom positions from a final Fourier synthesis could be used to define the model orientation. Residual peaks were *ca.* 1.0 e Å^{-3} for (**1**)—(**3**) and (**5**), and *ca.* 2 e Å^{-3} for (**4**); they were located in the vicinity of the metal atoms. All calculations were performed with the SHELX[13b] package of crystallographic programs. The co-ordinates of all non-hydrogen atoms are reported in Tables 7—11.

Addition material available from the Cambridge Crystallographic Data Centre comprises H-atom co-ordinates, thermal parameters, and remaining bond lengths and angles.

Acknowledgements

We thank the Ministero della Pubblica Istruzione and the Italian C.N.R. for financial support.

References

1 Part 2, B. T. Heaton, L. Strona, S. Martinengo, D. Strumolo, V. G. Albano, and D. Braga, *J. Chem. Soc., Dalton Trans.*, 1983, 2175.

2 V. G. Albano, M. Sansoni, P. Chini, and S. Martinengo, *J. Chem. Soc., Dalton Trans.*, 1973, 651.

3 Part 1, V. G. Albano, D. Braga, S. Martinengo, P. Chini, M. Sansoni, and D. Strumolo, *J. Chem. Soc., Dalton Trans.*, 1980, 52.

4 S. Martinengo, D. Strumolo, P. Chini, V. G. Albano, and D. Braga, *J. Chem. Soc., Dalton Trans.*, 1984, 1837.

5 A. F. Wells, 'Structural Inorganic Chemistry,' Clarendon Press, Oxford, 1975.

6 D. Braga and T. F. Koetzle, *J. Chem. Soc., Chem. Commun.*, 1987, 144.

7 D. E. Evans and D. M. P. Mingos, *J. Organomet. Chem.*, 1982, **232**, 171.

8 S. Martinengo, D. Strumolo, and P. Chini, *Inorg. Synth.*, 1980, **20**, 212.

9 F. Cariati and L. Naldini, *Gazz. Chim. Ital.*, 1965, **95**, 3.

10 B. K. Teo and J. C. Calabrese, *J. Am. Chem. Soc.*, 1975, **97**, 1256.

11 C. Cowala and J. M. Swan, *Aust. J. Chem.*, 1966, **19**, 547.

12 N. Walker and D. Stuart, *Acta Crystallogr., Sect. A*, 1983, **39**, 158.

13 G. M. Sheldrick, (*a*) SHELX 86, Crystal Structure Solution Program, University of Göttingen, 1986; (*b*) SHELX 76, System of Computer Programs, University of Cambridge, 1976.

Received 25*th March* 1987; *Paper* 7/539